Friction-Stir Processing

M.W. Mahoney[1] and S.P. Lynch[2]

[1] Manager Senior Scientist, Rockwell Scientific Company LLC, Thousand Oaks, Ca 91360, USA, mmahoney@rwsc.com
[2] Defence Science and Technology Organisation, Melbourne, Vic. 3001, Australia Stan.Lynch@dsto.defence.gov.au

Abstract

Friction-stir processing (FSP) is an emerging surface-engineering technology that can locally eliminate casting defects and refine microstructures, thereby improving strength and ductility, increase resistance to corrosion and fatigue, enhance formability, and improve other properties. FSP can also produce fine-grained microstructures through the thickness to impart superplasticity. The technology involves plunging a rapidly rotating, non-consumable tool, comprising a profiled pin and larger diameter shoulder, into the surface and then traversing the tool across the surface. Large surface areas can be traversed rapidly by using the appropriate tool design accompanied by rastering. Frictional heating and extreme deformation occurs causing plasticised material (constrained by the shoulder) to flow around the tool and consolidate in the tool's wake. FSP zones can be produced to depths of 0.5 to 50mm, with a gradual transition from a fine-grained, thermodynamically worked microstructure to the underlying original microstructure.

FSP has been applied to Al, Cu, Fe, and Ni-based alloys with resulting property improvements. Details of the benefits and limitations of FSP, along with examples of current and potential applications are presented below. Some examples of benefits include (1) a doubling of strength of cast nickel-aluminium-bronze, (2) a five-fold increase in ductility of Al alloy A356, (3) increased fatigue life by friction stir processing the surface of fusion welds, (4) depending on the microstructure, a 3 to 20 times increase in the corrosion resistance of a Cu-Mn alloy, and (5) bending of 25 mm thick 2519 Al plate to 85˚ at room temperature without surface cracking. The additional advantages of low-plasticity burnishing (LPB) following FSP, to change any residual near-surface tensile stresses introduced by FSP to compressive residual stresses, are also discussed.

Background

Friction stir processing (FSP) provides the ability to thermomechanically process selective locations on the structure's surface and to some considerable depth (>25mm) to enhance specific properties. This is accomplished by modifying technology developed for friction stir welding (FSW). Friction stir welding, a solid state joining process invented at TWI in 1991, is a viable technique for joining Al alloys that are difficult to fusion weld.[1-10] FSP uses the same methodology as friction stir welding (FSW), but FSP is used to modify the local microstructure and does not join metals together. A schematic illustration of FSP is shown in Figure 1. To friction process a location within a plate or sheet, a specially designed cylindrical tool is rotated and plunged into the selected area. The tool has a small diameter pin with a concentric larger diameter shoulder. When descended to the part, the rotating pin contacts the surface and rapidly friction heats and softens a small column of metal. The tool shoulder and length of entry probe control the penetration depth.

When the shoulder contacts the metal surface, its rotation creates additional frictional heat and plasticizes a larger cylindrical metal column around the inserted pin. The shoulder provides a forging force that contains the upward metal flow caused by the

Report Documentation Page

Form Approved
OMB No. 0704-0188

Public reporting burden for the collection of information is estimated to average 1 hour per response, including the time for reviewing instructions, searching existing data sources, gathering and maintaining the data needed, and completing and reviewing the collection of information. Send comments regarding this burden estimate or any other aspect of this collection of information, including suggestions for reducing this burden, to Washington Headquarters Services, Directorate for Information Operations and Reports, 1215 Jefferson Davis Highway, Suite 1204, Arlington VA 22202-4302. Respondents should be aware that notwithstanding any other provision of law, no person shall be subject to a penalty for failing to comply with a collection of information if it does not display a currently valid OMB control number.

1. REPORT DATE	2. REPORT TYPE	3. DATES COVERED
2006	**N/A**	**-**

4. TITLE AND SUBTITLE	5a. CONTRACT NUMBER
Friction-Stir Processing	5b. GRANT NUMBER
	5c. PROGRAM ELEMENT NUMBER
6. AUTHOR(S)	5d. PROJECT NUMBER
	5e. TASK NUMBER
	5f. WORK UNIT NUMBER
7. PERFORMING ORGANIZATION NAME(S) AND ADDRESS(ES) **Rockwell Scientific Company LLC, Thousand Oaks, Ca 91360**	8. PERFORMING ORGANIZATION REPORT NUMBER
9. SPONSORING/MONITORING AGENCY NAME(S) AND ADDRESS(ES)	10. SPONSOR/MONITOR'S ACRONYM(S)
	11. SPONSOR/MONITOR'S REPORT NUMBER(S)

12. DISTRIBUTION/AVAILABILITY STATEMENT
Approved for public release, distribution unlimited

13. SUPPLEMENTARY NOTES
The original document contains color images.

14. ABSTRACT

15. SUBJECT TERMS

16. SECURITY CLASSIFICATION OF:			17. LIMITATION OF ABSTRACT	18. NUMBER OF PAGES	19a. NAME OF RESPONSIBLE PERSON
a. REPORT	b. ABSTRACT	c. THIS PAGE			
unclassified	**unclassified**	**unclassified**	**UU**	**14**	

Standard Form 298 (Rev. 8-98)
Prescribed by ANSI Std Z39-18

tool pin. During FSP, the area to be processed and the tool are moved relative to each other such that the tool traverses, with overlapping passes, until the entire selected area is processed to a fine grain size. The rotating tool provides a continual hot working action, plasticizing metal within a narrow zone, while transporting metal from the leading face of the pin to its trailing edge. The processed zone cools, without solidification, as there is no liquid, forming a defect-free recrystallized, fine grain microstructure. Essentially, FSP is a local thermomechanical metal working process that changes the local properties without influencing properties in the remainder of the structure.

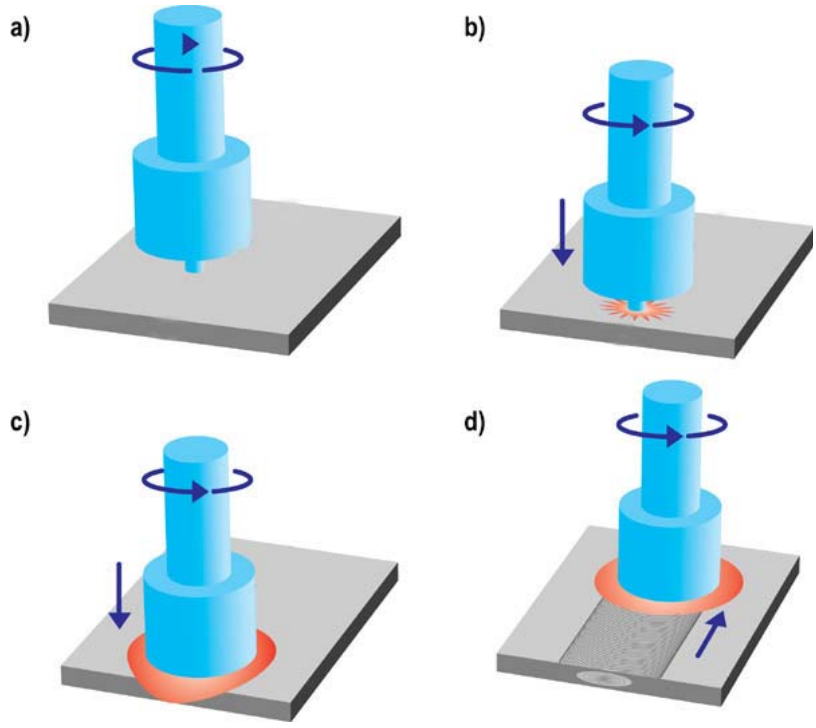

Figure 1 Schematic illustration of friction stir processing: a) rotating tool prior to contact with the plate; b) tool pin makes contact with the plate, creating heat; c) shoulder makes contact, restricting further penetration while expanding the hot zone; and d) plate moves relative to the rotating tool, creating a fully recrystallized, fine grain microstructure.

Increased strength in cast NiAl bronze

Microstructural Evolution. The three dominant microstructures created in NiAl bronze (NAB) by FSP are illustrated in Figures 2a-2c and are in sharp contrast to the coarse as-cast NAB microstructure illustrated in Figure 2d. Details of these FSP microstructures are presented elsewhere including orientation imaging analysis, transmission electron microscopy, and discussions of the microstructural and second phase evolution.[11] Presented herein is a macro description of these microstructures sufficient to correlate with mechanical properties. Figure 2a illustrates a lamellar or banded microstructure. The bands consists of α (white areas), and martensite containing Widmanstäten α (dark areas).[11] The bands are elongated in a horizontal direction, perpendicular to the tool rotation axis. Figure 2b illustrates a recrystallized, equiaxed fine grain microstructure likely with the same phases present as with the lamellar structure but as discreet grains as opposed to the bands. However, this microstructure also shows a phase orientation bias in the horizontal direction. Figure 2c illustrates a Widmanstäten or basket weave microstructure. There does not appear to be any macro orientation bias with the

Widmanstäten microstructure. For mini tensile samples (1 mm gage length), the tensile axis was taken horizontal to the micrographs in Figure 2, i.e., micro tensile samples were oriented in the long traverse direction in the FSP plate or normal to the axis of the FSP tool.

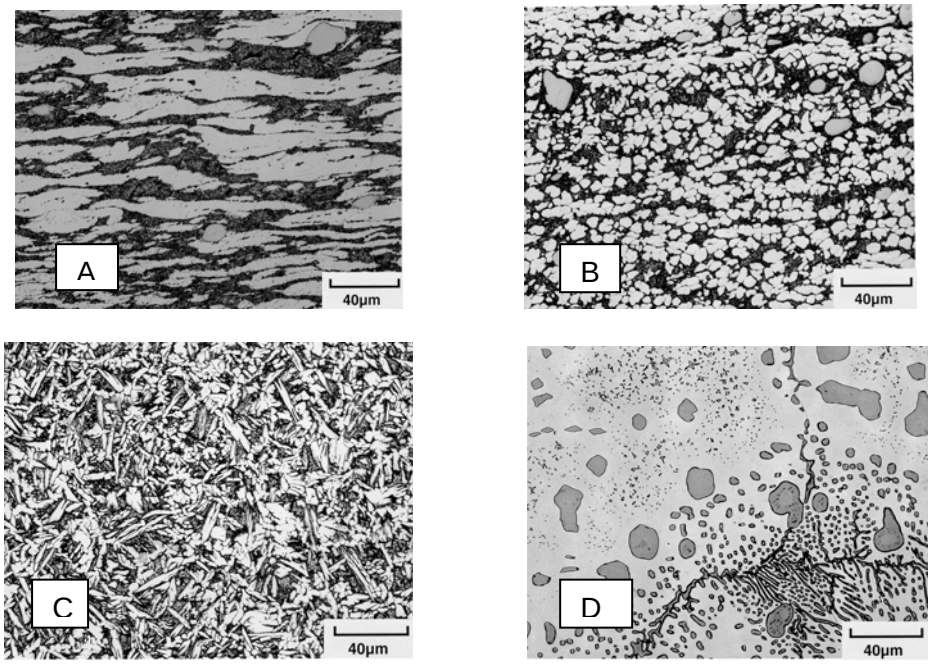

Figure 2 Microstructures created in NiAl bronze by friction stir processing.
a) Lamellar, b) fine grain, c) Widmanstäten, and d) as-cast.

Mechanical Properties. Table 1 tabulates hardness and mechanical property results for the different FSP microstructures created in NAB. These results are from both mini-tensile samples, to determine properties from different microstructures, and from larger bulk samples to determine composite properties. As-cast results are for an average of six samples using round-bar tensile samples of diameter 3 mm. Due to the casting defects and significant chemical segregation in the as-cast NAB, it is difficulty to obtain consistent results with the small gage section used for the mini-tensile tests. However, even with different test sample geometries, a comparison between as-cast and FSP results represent real property differences. For example, as shown below, test results are equivalent for both the mini and bulk test sample geometries for the FSP Widmanstäten microstructure (compare lines C and F in Table 1).

Table 1 Hardness and mechanical properties for friction stir processed NiAl bronze.

Line	Microstructure NAB	Hardness RB	Elongation (%)	Yield Strength (MPa)	Tensile Strength (MPa)
D	As-Cast (1)	68-75	20	214	445
A	Lamellar	92	----	480	756
B	Fine Grain	91	23	508	776
C	Widmanstäten	93	20	572	823
E	Composite of All Microstructures	X	23	433	741
F	Widmanstäten	93	24	591	824

Lines A, B, and C are properties developed with mini-tensile samples with gage area 0.5 mm^2. Lines D, E, and F are properties developed with 3 and 6 mm diameter tensile bars. Lines A, B, and C illustrate properties in the long transverse direction for individual microstructures. Line D illustrates properties for the as cast NiAl bronze. Line E illustrates properties for a composite of the three microstructures. Line F illustrates properties for the Widmanstäten microstructure for a large cross-section.

Hardness results illustrate a significant difference between the as cast and FSP microstructures (RB hardness 71 vs. 92) but do not differentiate between the different FSP microstructures. This result is not surprising. With the refined microstructures and the number of phases present in each microstructural morphology, even micro-hardness hardness results are likely measuring hardness in a composite of phases.

In all cases, elongation is high. The average elongation to failure for the as-cast NAB was 20%; albeit, due to casting defects and the inhomogeneous microstructure, the ductility at times can be significantly lower. Following FSP, the strain to failure remains high and as shown in Table 1, for some microstructures even increases. This is especially true for the larger diameter samples where elongation was consistently greater than 23%. For the banded microstructures, i.e., lamellar and fine grain, ductility results could be different if testing was performed normal to the banding.

Yield and tensile strengths for the as-cast NAB are 214 MPa and 445 MPa respectively. In comparison, following FSP and for the mini-tensile samples, lines A and B, table 1, yield strength more than doubles and tensile strength increases from 70% to 85% for the lamellar and fine grain microstructures. Strengths for the lamellar and fine grain microstructures are similar. We speculate that these results reflect the apparent banding of the fine α-grains and perhaps with more mixing during FSP, strength could increase even more with the fine grain microstructure. Mechanical properties of the Widmanstäten microstructure are the highest for the mini-tensile sample; line C, table 1. Yield strength increases by a factor of 1.7 and tensile strength increases by 85%. These dramatic property increases reflect the fine homogeneous microstructure and the absence of casting porosity following friction stir processing.

As shown in the macrograph in Figure 3, a composite of microstructures can be created by FSP. Round tensile bars were machined to include all the microstructures in the gage diameter, i.e., lamellar, fine grain, and Widmanstäten. For a range of processing parameters and tool geometries, average elongation for twelve samples was high at 23%, yield strength was 433 MPa, and tensile strength 741 MPa; line E, table 1. This is a significant increase over the as-cast NAB, but mechanical properties are less than that demonstrated for the single Widmanstäten microstructure using a mini-tensile sample; line C, table 1. This illustrates the influence of the “weaker” microstructures on mechanical properties. Thus, to maximize strength it would be preferable to create a single, homogeneous Widmanstäten microstructure. Figure 4 illustrates a 27 mm deep FSP zone created with two passes where a homogeneous Widmanstäten microstructure was created. The corresponding properties for this sample include a strain to failure of 24%, yield strength of 591 MPa, and a tensile strength of 824 MPa, line F, table 1. These results are essentially equivalent to the mechanical properties demonstrated with the mini tensile samples for this same microstructure.

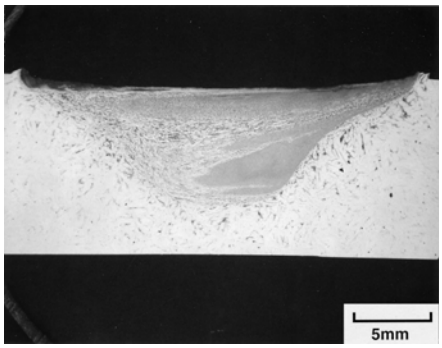

Figure 3 Friction stir processed zone in NiAl bronze illustrating a composite of Microstructures.

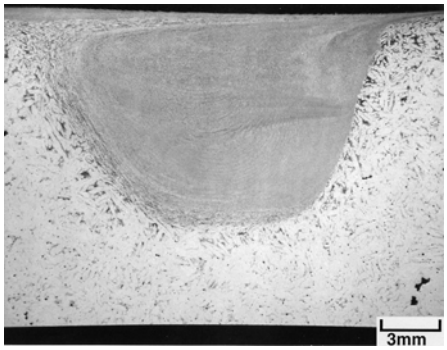

Figure 4 Friction stir processed zone in NiAl bronze with a homogeneous Widmanstäten microstructure.

Enhanced ductility in cast A356 aluminum

Typically, aluminum castings contain porosity, segregated chemistries, and inhomogeneous microstructures, Figure 5a. These undesirable features result in property degradation including reduced strength and ductility, poor corrosion resistance, and limited fatigue life. Following FSP, casting porosity is eliminated and a relatively homogeneous, fully recrystallized fine grain microstructure is created, (Figure 5b). In concert with the FSP microstructure, mechanical property improvements are also achieved. As shown in Figure 6, tensile strength is increased to 34 MPa (an 18% increase) and strain to failure increased from 3% to 17%. It is not practical to FSP an entire, complex shaped casting. However, at selected locations where property improvements could enhance the service life or performance of a structure, it would be possible to "locally" FSP. For example, if an attachment point was required, and this location was loaded in service, an increase in ductility would be necessary. FSP could be applied to an appropriate depth providing a ductile microstructure with increased tensile strength. In aluminum alloys, FSP can be applied to the surface to a depth as low as approximately 0.5 mm or as deep as 50 mm.

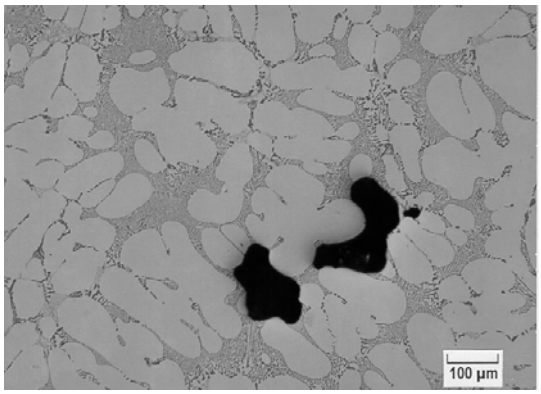

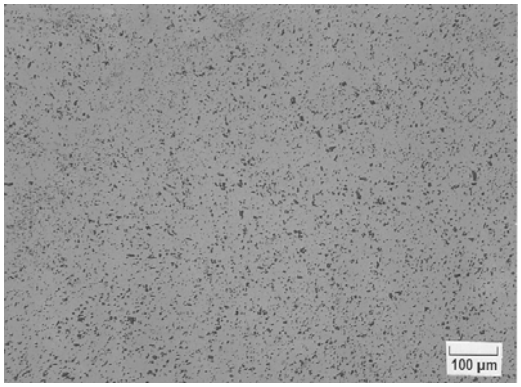

(a) (b)

Figure 5 (a) As-cast A356 Al illustrating casting porosity and a dendritic microstructure, and (b) FSP A-356 showing a homogeneous microstructure.

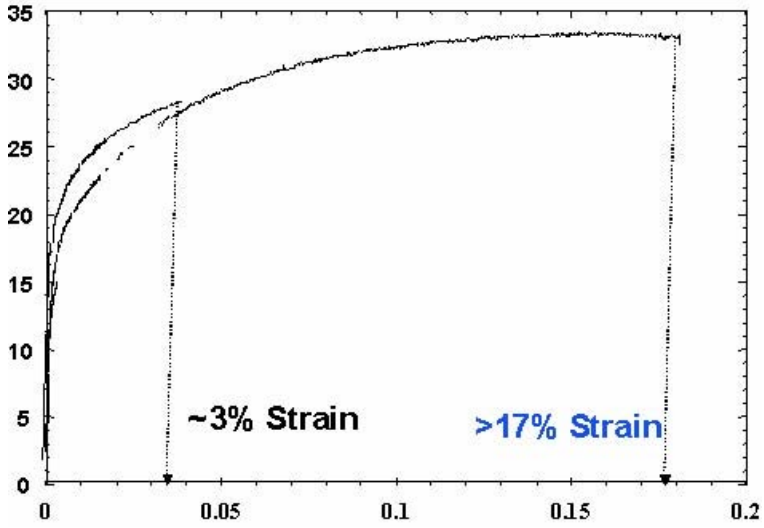

Figure 6 Stress/strain behavior of as-cast A356 aluminum and the same alloy following friction stir processing.

Increased fatigue life in 5083-H321 aluminum fusion welds

It will not be possible to friction stir weld all aluminum structures and reap the benefits of this solid state process. For example, large structures, inaccessible locations, and very thick plate would be difficult to friction stir weld. However, eventually it may be possible to friction stir process the surface of fusion welds using a portable system. By friction stir processing the surface, the cast fusion weld microstructure will be converted to a fully recrystallized fine grain and weld defects near the surface will be eliminated. Potential benefits include both increased corrosion resistance and fatigue life. The following illustrates an example whereby the crown or toes of a fusion weld are friction stir processed and subsequent fatigue life increased.

Automated metal inert gas (MIG) welding of 6 mm thick 5083-H321 Al was performed parallel to the longitudinal direction of rolled plates using a 5356 Al weld filler alloy. FSP used two different tools, i.e., a tool with a small diameter shoulder and a customized pin and a tool with a larger diameter scrolled shoulder and the same shape of customized pin with a shorter length. The small diameter shoulder tool was designed for a single FSP pass along each of the two fusion weld toes (interface between fusion weld and parent material on the top surface), producing a total of two FSP passes per plate. The larger diameter scrolled shoulder tool was designed for a single FSP pass across the entire fusion weld crown. FSP was performed with the FSP tool operating in Z-axis load control. Four FSP conditions were examined including 1) as-fusion welded, 2) small shoulder tool with the fusion weld on the advancing side of the FSP tool, 3) small shoulder tool with the fusion weld on the retreating side of the FSP tool, and 4) a large shoulder tool.

Figures 7a-7d illustrate light macrographs taken in the short-transverse direction (perpendicular to the fusion weld) for the four FSP conditions, i.e., (a) as welded, (b) small shoulder tool with fusion weld on advancing side, (c) small shoulder tool with fusion weld on retreating side, and (d) large shoulder tool. The FSP tool travel direction is into the page, and the advancing side of the tool is on the right-hand side (counter-clockwise tool rotation). Figure 7 illustrates the three microstructural regions observed in this study, i.e., fusion weld, parent material (PM), and fine-grain FSP; indicated by 1, 2, or 3, respectively.

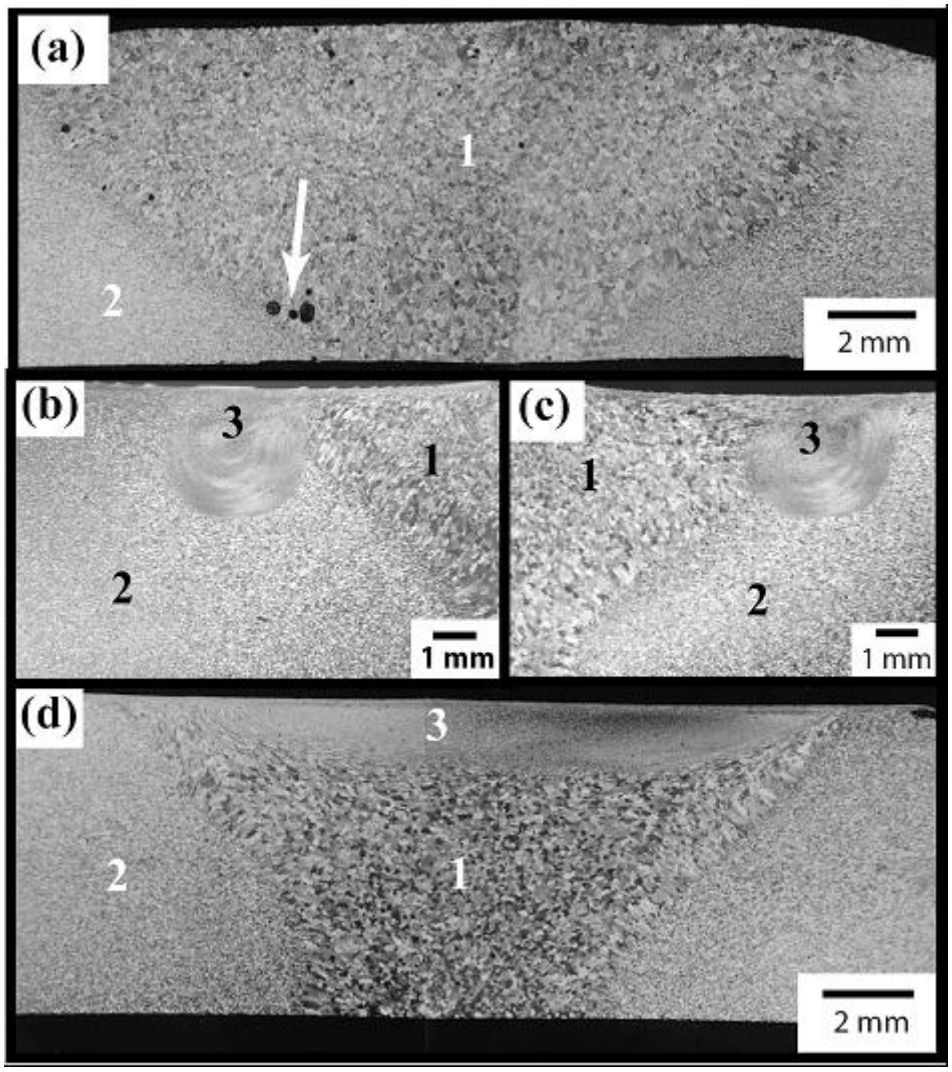

Figure 7 Light macrographs of 5083-H321 Al in the following conditions: a) as-fusion welded, (b) small shoulder tool with fusion weld on advancing side, (c) small shoulder tool with fusion weld on retreating side, and (d) large shoulder tool. Different microstructural regions within the micrographs are indicated by 1) fusion weld (5356 Al), 2) parent material (5083 Al), and 3) fine-grain FSP. The arrow in (a) indicates porosity within the fusion weld. The right-hand side is the advancing side of the FSP tool, and the direction of tool travel is into the page.

The fusion weld region has a coarse-grain microstructure comparable to that of a cast alloy. As seen in the cast microstructure, porosity is present in the fusion weld, arrow in Figure 7a. The fine equiaxed grains observed in the FSP region are the result of mixing both the fusion weld and parent metal alloys. Intimate mixing of the fusion weld metal (5356 Al) with the parent metal (5083-T321 Al) is observed for all FSP conditions, Figures 7b-7d. Significant differences in the profiles of the small shoulder tool as a function of fusion weld location (advancing side vs. retreating side) are not observed with light microscopy. The small shoulder tool also produces the commonly observed “onion ring” structure, Figures 7b and 7c. However, the “onion ring” structure is not observed with the large shoulder tool, Figure 7d, due to the design of the scrolled shoulder and customized pin.

Fatigue tests were performed transverse to the weld direction for these three different microstructural conditions in four point bending using R=0.1. Test results are illustrated in Figure 8. Considering run out as 10^7 cycles, these results illustrate a 30% increase in run out stress following FSP. These results show the significant benefits of modifying the fusion weld surface using FSP. There was no difference in fatigue life for FSP of the weld toes versus FSP of the entire weld crown. However, each approach offers different benefits. For example, using the small tool to FSP the weld toes, the applied vertical load was considerably less than that for the large tool used to FSP the weld crown. Low loads are important for design of a portable FSP system that will be required to react the FSP loads. However, FSP of the separate toes requires two passes whereas processing of the entire crown can be completed in one pass.

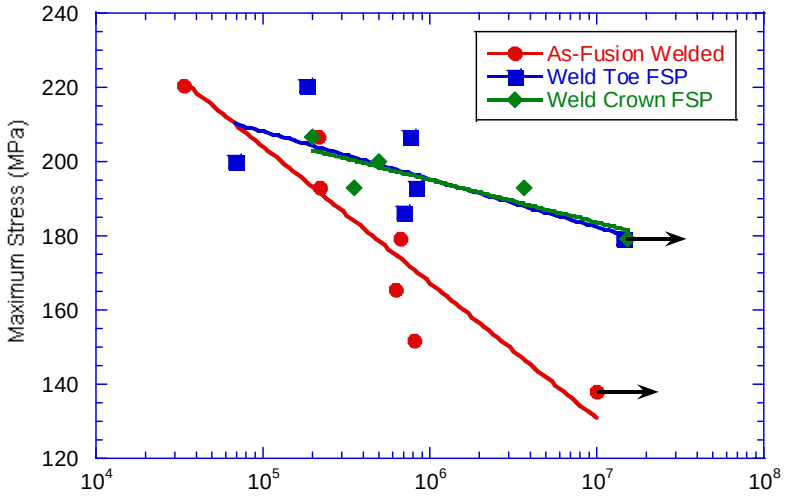

Figure 8 Fatigue life of fusion welded 5083-H321 aluminum and the same alloy following friction stir processing of the weld crown or the weld toes.

Corrosion resistance in a Cu-Mn alloy

Friction stir processing was applied to cast Sonoston, a 52Mn-4Al-3Fe-1.5Ni-39Cu alloy commonly used in a seawater environment. The cast Sonoston microstructure is relatively coarse and suffers from selective de-alloying. Friction stir processing was evaluated to determine if corrosion resistance could be increased by refining the microstructure. As with the NiAl bronze, a variety of microstructures are created by FSP. For FSP material (~0.1mm below the FSP surface) with a refined Widmanstätten microstructure, de-alloying in sea water for 24hrs at –200mV occurred to similar depths to as-cast material. However, for the FSP material, much more severe cracking (delamination parallel to the surface as well as normal to the surface) occurred, and surface layers 'flaked-off' readily (Figure 9). Similar depths of de-alloying and cracking behavior were observed for surfaces with mixtures of fine and coarse plates towards the edges of the FSP zone just beneath the FSP surface (Figure 10). Specimens with surfaces exhibiting a very fine-grained microstructure (~4mm below the original FSP surface) were also de-alloyed and cracked to a depth of about 400μm after exposure to sea water for 24hrs at –200mV (Figure 11).

After stress-relieving heat-treatments, the depths of de-alloying for the refined FSP microstructures were substantially reduced compared with the coarse as-cast

structure. For the fine Widmanstätten microstructure just below the FSP surface, stress-relieving for various times and temperatures showed that 8hrs at 500ºC or 24hrs at 600ºC were required for improved corrosion resistance (Figure 12). For specimens with the fine-grained region at the surface, 24hrs at 450ºC was sufficient to dramatically decrease the depth of de-alloying (to only 5-10μm) (Figure 13). The stress-relief heat-treatments appeared to have little effect on the depth of de-alloying for the coarse as-cast microstructures.

The stress-relieved and refined FSP microstructures have shallower de-alloyed layers than the coarse as-cast microstructures because de-alloying is confined to Mn-rich regions that are connected to the surface, and such regions occur to shallower depths following FSP. However, when high residual tensile stresses are present (created by FSP), SCC occurs through the Cu-rich areas, thereby allowing the environment to penetrate to Mn-rich areas not otherwise connected to the surface, so that de-alloying continues to occur. A somewhat lower stress-relief temperature for the fine-grained microstructure compared with the refined Widmanstätten microstructure is required possibly because residual stresses were lower at greater depths below the FSP surface or because the fine-grained microstructure is inherently more resistant to SCC (or both).

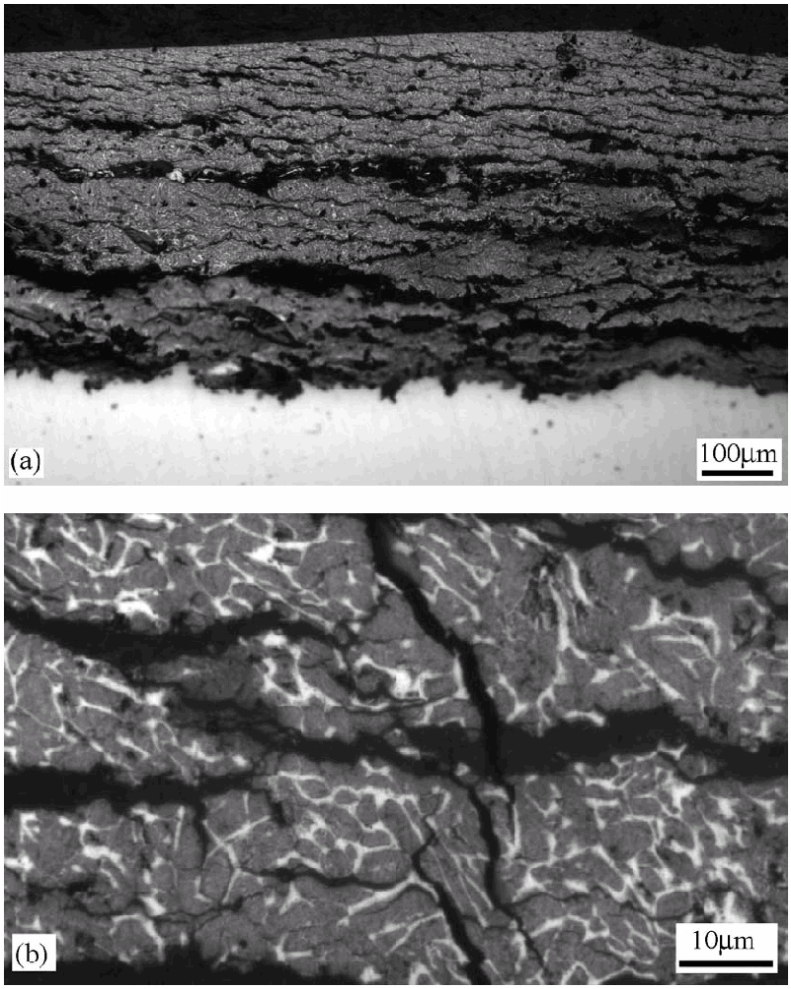

Figure 9 Optical micrographs of *unetched sections* normal to the surface of specimens with the CBN-FSP fine Widmanstätten microstructure dealloyed for 24hrs at –200mV in sea water, (a) at low magnification showing heavily cracked de-alloyed layer, and (b) at high magnification showing de-alloyedMn-rich areas and uncorroded Cu-rich areas.

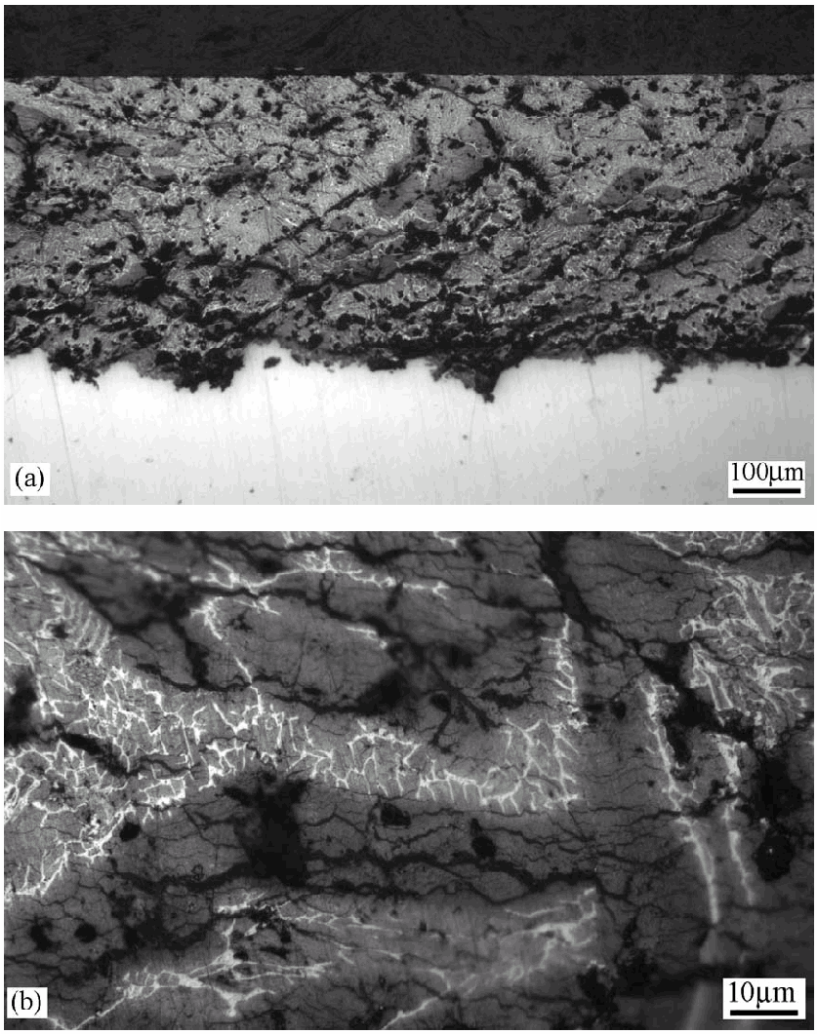

Figure 10 Optical micrographs of *unetched sections* normal to the surface of specimens with the CBN-FSP fine and coarse Widmanstätten, de-alloyed for 24hrs at –200mV in sea water (a) at low magnification, and (b) at high magnification.

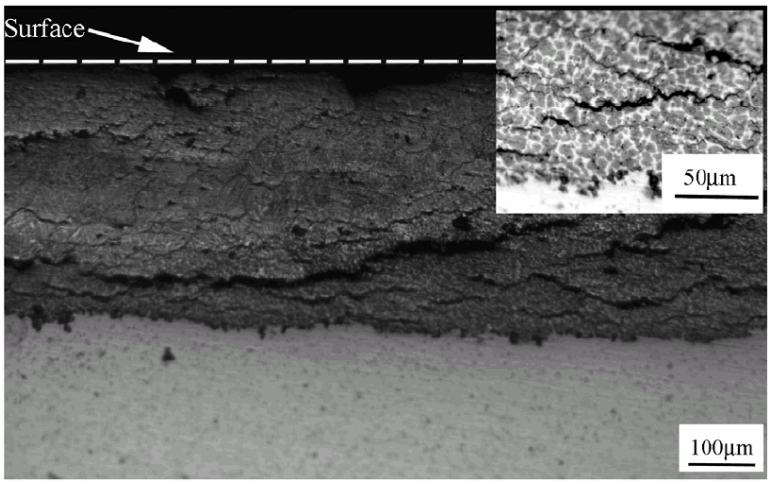

Figure 11 Optical micrograph of *unetched section* normal to the surface of specimen with the CBN-FSP fine grained microstructure (4mm below FSP surface) after de-alloying for 24hrs at –200mV, inset shows high magnification view.

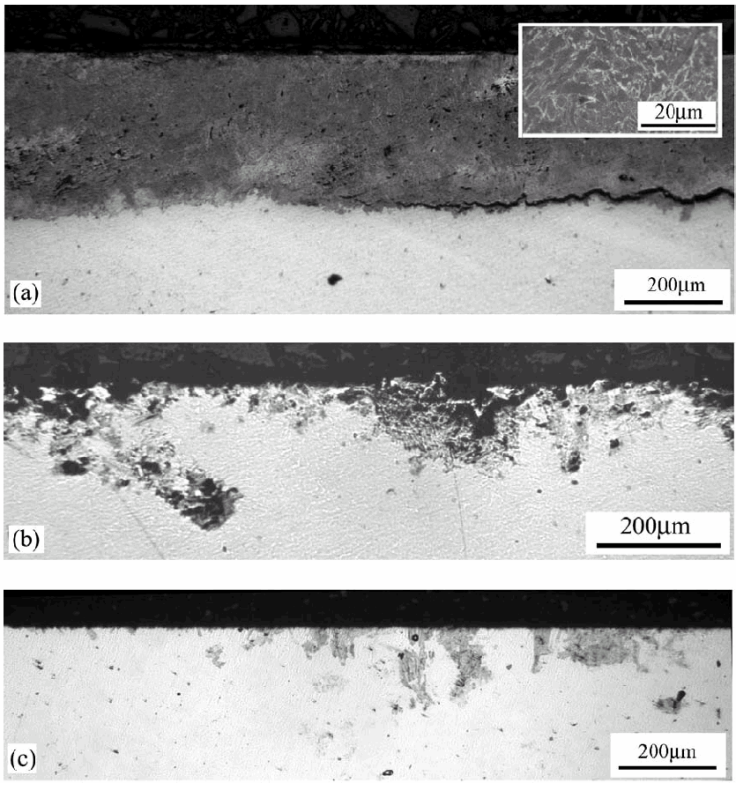

Figure 12 Optical micrographs of *unetched sections* normal to surface with a CBN-FSP fine Widmanstätten structure de-alloyed for 24hrs at –200mV (versus saturated calomel electrode) specimens stress-relieved for: (a) 24hrs at 450ºC, (b) 8hrs at 500ºC, and (c) 2hrs at 600ºC.

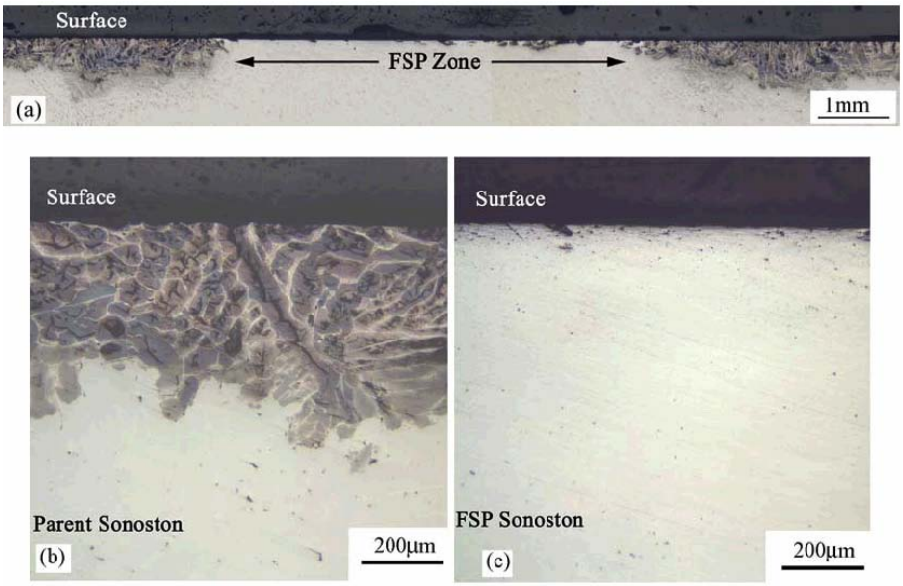

Figure 13 Optical micrographs of unetched sections normal to surfaces with CBN-FSP fine-grained globular structures, and adjacent as-cast structures de-alloyed for 24hrs at –200mV (versus SCE) for specimens stress-relieved for 24hrs at 450ºC. (a) FSP zone and adjacent as-cast zones at low magnification and (b), (c) FSP zones and adjacent zones at a higher magnification.

Room temperature bending of 25mm thick 2519 aluminum

Friction stir processing can also be used to enhance the formability of aluminum alloys. A number of authors have demonstrated exceptional superplasticity following FSP.[12-14] However, superplastic forming requires high temperature and the aluminum is friction stir processed through the entire sheet thickness. A different surface engineering application for FSP is the creation of room temperature formability in thick aluminum plate. For this application of FSP, a large surface area is friction stir processed. This is accomplished by rastering the FSP tool forward and back until the surface area that subsequently experiences high tensile stresses during bending has been processed. Typically, the FSP tool is moved ½ pin diameter to the advancing side of the previous pass. FSP provides three changes including 1) creation of a fine grain microstructure with increased ductility, 2) the surface is essentially annealed without significantly changing properties of the unprocessed metal, and 3) any superficial surface cracks associated with plate processing are removed. Figure 13 illustrates an example whereby the FSP tool pin penetrated 6 mm into a 25 mm thick 2519 aluminum plate. Following FSP, the plate was bent at room temperature to 80º without cracking. For comparison, as-received plate was bent using the same procedure and failed after approximately 30º. This FSP/bending process could replace conventional techniques where a structure is fabricated by fusion welding thick plates into a complex shape.

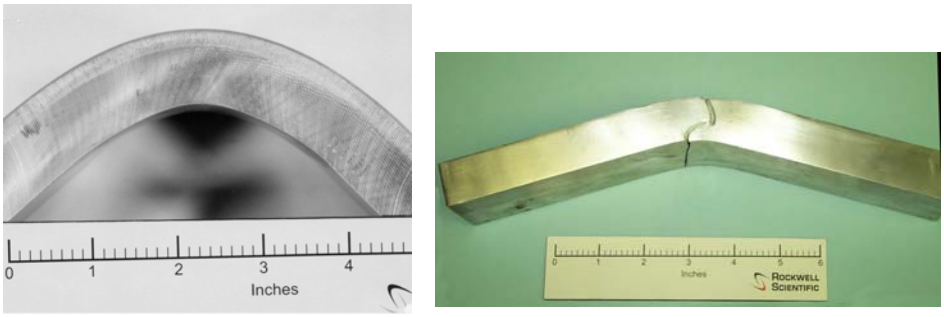

Figure 13 a) Room temperature bending of 25 mm thick 2519 aluminum plate to 80º following FSP to a depth of 6 mm, and b) fracture of as-received plate at a 30º bend.

FSP and low plasticity burnishing to increase corrosion fatigue strength

Friction stir processing locally creates a high temperature, short time, thermal transient. Like any high temperature process, this can result in tensile residual stresses on the structure's surface. To change FSP tensile residual stresses to compressive, low plasticity burnishing (LPB) has been explored. Figure 14 is a photograph of LPB in operation on a CNC milling machine. Briefly, LPB produces a layer of compressive residual stress of high magnitude and depth with minimal cold work.[15-18] LPB is usually performed using a single pass of a smooth free rolling ball under a normal force sufficient to plastically deform the surface of the material. Hertzian loading creates a layer of compressive residual stress to a depth as much as 4 mm. The ball is supported in a fluid bearing with sufficient pressure to lift the ball off the surface of the retaining spherical socket. The ball is in solid contact only with the surface to be burnished and is free to roll on the surface of the work piece. LPB parameters were optimized for the 2219-T8751 friction stir weld, i.e., to impart the greatest depth and magnitude of residual stress with minimal cold work. For this work, the LPB was performed in the direction of the weld using multiple passes adjacent to and in the weld.

Low plasticity burnishing produced compressive residual stresses as high as –450 MPa both parallel to and perpendicular to the weld direction. This compares to a tensile residual stress greater than +200 MPa in the as-friction stir welded sample. Figure 15 illustrates fatigue and corrosion/fatigue results for friction stir welded 2219 aluminum in the following conditions: 1) milled, 2) milled + LPB, 3) milled + 100 hours in a salt environment, and 4) milled + LPB + 100 hours in a salt environment. LPB increased the endurance limit by nominally 60% in salt corroded FSW specimens. Specimens that were LPB and salt corroded had the same nominal fatigue strength as samples that were LPB processed without corrosion indicating that LPB process eliminated any fatigue debit from salt fog corrosion.

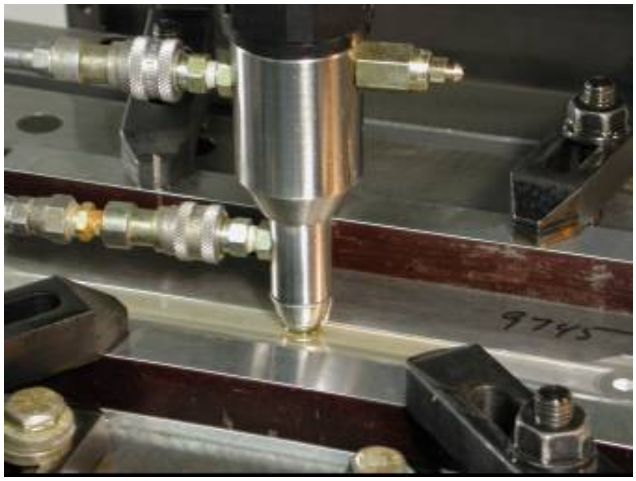

Figure 14 Low plasticity burnishing of a FSP 2219 aluminum plate.

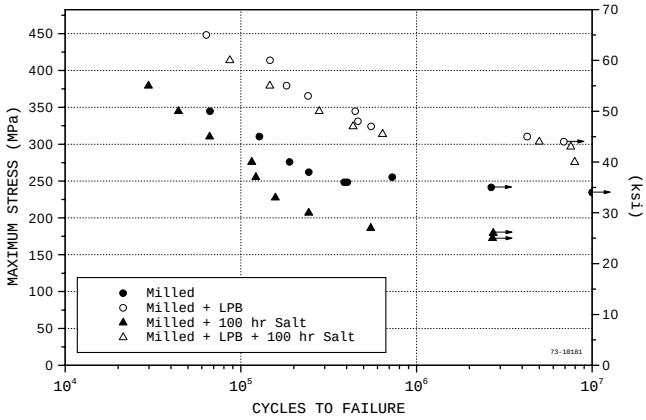

Figure 15 Fatigue and corrosion/fatigue test results fro friction stir welded 2219-T8751 aluminum with and without low plasticity burnishing.

Acknowledgements
The authors would like to recognize the support of other contributors to this work including Christian Fuller of RSC for thick section bending and FSP modification of fusion welds, Paul Prevéy and Doug Hornbach of Lambda Research for their work on low plasticity burnishing, Rajiv Mishra of the University of Missouri for micro mechanical testing, and William Bingel and Mike Calabrese of RSC for laboratory and metallographic support. The authors also acknowledge DARPA for supporting this work under contract No. MDA972-02-C-0030.

References

[1]. W.M. Thomas, et al, “Friction Stir Butt Welding”, International Patent Appl. No. PCT/GB92/02203, GB Patent Appl. No. 9125978.8, Dec. 1991, and U.S. Patent No. 5,460,317, Oct. 24, 1995.

[2]. C.J. Dawes and W.M. Thomas, *TWI Bulletin 6*, (Nov./Dec. 1995)p. 124.

[3]. M. Ellis and M. Strangwood, *TWI Bulletin 6*, (Nov/Dec 1995): p. 138.

[4]. C.J. Dawes and W.M. Thomas, *Welding Journal*, 75, (1996): p. 41.

[5]. O.T. Midling, “Material Flow Behavior and Microstructural Integrity of Friction Stir Butt Weldments”, *Proc. 4th Int'l. Conf. on Aluminum Alloys*, Atlanta GA, (Sept. 1994).

[6]. M.W. Mahoney, *Welding and Joining*, (Jan/Feb 1997): p. 18-20.

[7]. S. Kallee and D. Nicholas, *Welding and Joining*, (Feb. 1998): p. 18-21.

[8]. C. J. Dawes, *Welding & Metal Fabrication*, (January 1995): p. 14-16.

[9]. C.G. Rhodes, M.W. Mahoney, W.H. Bingel, R.A. Spurling, and C.C. Bampton, *Scripta Met*., 36 (1997): p. 69.

[10]. M.W. Mahoney, C.G. Rhodes, J.G. Flintoff, R.A. Spurling, and W.H. Bingel, *Metallurgical and Materials Transactions A,* vol. 29A (1998): p. 1955.

[11]. K. Oh-ishi, A.M. Cuevas, D.L. Swisher, and T. McNelley, Proceedings of THERMEC 2003, International Conference on Processing & Manufacturing of Advanced Materials, Leganès, Madrid, Spain, July 7-11, 2003.

[12]. R. Mishra, M. Mahoney, S. McFadden, N. Mara, and A. Mukheerjee, Scripta Mater. 42 (2000) 163-168.

[13]. M. Mahoney, R. Mishra, T. Nelson, J. Flintoff, R. Islamgaliev, and Y Hovansky, TMS Proceedings, Friction Stir Welding and Processing, Nov. 4-8, 2001, pp. 183-194.

[14]. I. Charit, R. Mishra, and K. Jata, TMS Proceedings, Friction Stir Welding and Processing, Nov. 4-8, 2001, pp. 225-234.

[15]. P. Prevéy, J. Telesman, T. Gabb, and P. Kantzos, Proc. 5th National High Cycle Fatigue Conference,Chandler, AZ, March 7-9, (2000).

[16]. J. Cammett and P. Prevéy, Proc. 4th International Aircraft Corrosion Workshop, Solomons, MD, Aug. 22-25, (2000).

[17]. P. Prevéy, M. Shepard, and P. Smith, Proc. 6th National Turbine Engine HCF Conference, Jacksonville, FL, March 5-8, (2001)

[18]. P. Prevéy and J. Cammett, Proc. 5th International Aircraft Corrosion Workshop, Solomons, MD., Aug. 20-23, (2002).